JOURNAL OF NANO- AND ELECTRONIC PHYSICS *ЖУРНАЛ НАНО- ТА ЕЛЕКТРОННОЇ ФІЗИКИ*
Vol. **14** No 1, 01029(5pp) (2022) Том **14** № 1, 01029(5cc) (2022)

Features of Noise Generation in Graded-Gap III Nitride-based Diodes

K.H. Prykhodko[1,*], S.V. Plaksin[2]

[1] *V.N. Karazin Kharkiv National University, 4, Svoboda Sq., 61077 Kharkiv, Ukraine*
[2] *Institute of Transport Systems and Technologies of NAS of Ukraine, 5, Pisarzhevsky St., 49005 Dnipro, Ukraine*

(Received 28 December 2021; revised manuscript received 21 February 2022; published online 28 February 2022)

The paper reports the result of our research on graded-gap diodes with a cathode static domain as possible noise sources for different modern applications based on the use of THz wave frequencies. Such diodes represent a two-terminal $n^+ - n^- - n - n^+$ structure containing a cathode graded-gap layer with a band gap that increases from the cathode contact towards the n-region. We study GaN and AlN based diodes with $In_zGa_{1-z}N$ and $In_zAl_{1-z}N$ based graded-gap layers, respectively. It is shown that the localization of a strong electric field and low values of impact ionization threshold can be achieved by using a graded-gap layer with a narrow-gap material on the cathode. The diode simulation is performed using ensemble Monte Carlo technique. Noise generation is investigated numerically with time sampling of electric current over the time domain. The influence of scattering mechanisms acting on charge carriers on the noise properties of the diode is explored. Analyzing the noise power spectral density (NPSD), it is found that maximum NPSD can be observed in GaN diodes with $In_zGa_{1-z}N$ layer, and the NPSD magnitude depends both on the size of the n^--region (at a fixed diode length) and on the position of the graded-gap layer with respect to the end of the high resistance region (n^-). It is established that polar phonon scattering and alloy-disorder scattering are the main mechanisms affecting the noise properties of the diodes. It is shown that the diodes demonstrate bias voltage regions where the dependence of NPSD on bias voltage is linear, and the value of NPSD increases by an order of magnitude.

Keywords: Cathode static domain, Graded-gap layer, Impact ionization, Noise generation, Scattering, Noise power spectral density.

DOI: 10.21272/jnep.14(1).01029 PACS numbers: 85.30.Fg, 73.40.Kp, 73.40. – c

1. INTRODUCTION

Terahertz noise sources are widely used for radiometric system calibration and other applications related to biological systems, object state monitoring [4] and others. Frequency ranges of SHF and EHF bands are mainly used [1-3] for these purposes. However, the radiometric aperture of sub-terahertz (sub-THz) range and the implementation of terahertz (THz) measurement systems are also in demand for research and development today. Nowadays, three-dimensional (3D) THz imaging or THz tomography [5-7] is of great interest, making the creation of noise sources in the sub-THz and THz ranges the actual task.

The main parameters of noise generators are noise power spectral density (NPSD) and output power in a given frequency band. NPSD must be uniform. It is necessary to obtain a large output power and ability of calibration and adjustment in the widest frequency range. Noise characteristics must be invariant and reproducible over time and under different external conditions. These requirements can be satisfied by using solid-state noise sources. Today, the most widely used devices are Schottky diodes [8], field effect transistors (FETs) [10] and avalanche diodes [9].

Impact ionization is the most applied effect in noise generation. For instance, the generation of noise and the operation of avalanche diodes are based on the impact ionization effect. Another diode based on the impact ionization effect is a diode with a cathode static domain [11, 12]. For instance, in [11], noise generation is obtained experimentally in GaAs-based diode in the X-band and is possible in the higher frequency range. The diode features are single-carrier-type conductivity and operation regime when the impact ionization process is at the initial stage, which can lead to a potentially better frequency response in comparison with avalanche diodes containing p-n junctions. $n^- - n$ junction is used to form a region with high electric field strength near the cathode called the cathode static domain (CSD), where charge carriers gain enough energy for the impact ionization effect. It is found that the noise properties of the diode are mainly determined by the parameters of CSD and transition of electron-hole pairs in the CSD region. So, the size of CSD strongly affects the spectral properties of the diode. This fact was accounted in graded-gap diode active elements, which were proposed earlier [13]. The diode has the $n^+ - n^- - n - n^+$ structure, where the graded-gap semiconductor layer is the $n^+ - n^-$ region. The material changes from a narrow-gap semiconductor at the cathode to a wide-gap one at the end of the graded-gap layer. In this way, the magnitude of the electric field corresponding to the impact ionization threshold is low, which provides a small region of strong electric field and higher operation frequencies. An example of such structures is InGaAs/GaAs-based diodes considered in [14]. It is shown that the diodes have better magnitude of NPSD in the THz frequency region compared to GaAs-based diodes, whose composition is uniform. The frequency parameters of a graded-gap layer strongly affect its frequency properties. Thus, their choice is important for obtaining the required frequency and power characteristics of the diode. Promising materials for graded-gap diodes are III-nitride compounds. Their advantage is the possibil-

*kyrylo.prykhodko@karazin.ua

ity to obtain a significantly larger quasi-electric field, mainly due to the use of InN at the cathode. The aim of our research is to analyze the electronic processes in CSD diodes based on InGaN/GaN and InAlN/AlN material systems and to determine the graded-gap layer parameters which affect the noise properties of the diodes.

2. DIODE STRUCTURE AND SIMULATION MODEL

2.1 Diode Structure

We consider graded-gap diodes with CSD of the $n^+ - n^- - n - n^+$ structure with two ohmic contacts and a total length of 1.28 μm and a graded-gap layer based on InGaN or InAlN, where In mole fraction decreases to zero in the direction from the cathode contact to the n^--n junction. The doping profile and compound composition $z(x)$ as a function of the x coordinate are shown in Fig. 1.

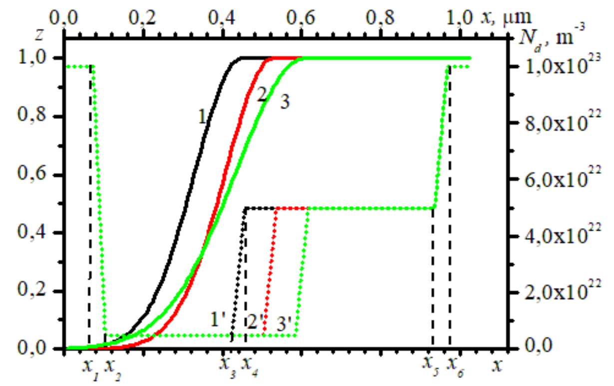

Fig. 1 – Doping profile and alloy composition $z(x)$ as a function of the x coordinate

The distributions of the alloy composition (mole fraction of indium) $z(x)$ representing Gaussian profiles are shown in Fig. 1. The region length of low n^- concentration was considered as a factor which directly affects the NPSD level. It was accounted by the n^- region size to n-region size ratio δ. The doping level in it was limited by intrinsic concentration of InN and was equal to $N_d = 10^{22}$ m^{-3}. Donor concentrations in the n-region and contact regions were $5 \cdot 10^{22}$ m^{-3} and 10^{24} m^{-3}, respectively.

The processes leading to noise generation in sub-THz and THz ranges are of main interest here because the noise oscillations are compatible on the time scale with the scattering times of electrons and holes. Thus, our goal is to obtain a close to real time dependence of the current through the diode, which must depict the stochasticity of the electronic process. We applied the synchronous Ensemble Monte Carlo (EMC) technique to achieve our goal. A three-valley model of the conduction band, represented by the lower Γ- and upper Γ_1- and M-L-valleys, was used to consider $Ga_zIn_{1-z}N$-based diodes and a two-valley model, represented by the lower Γ- and upper M-L-valleys, was used to consider $In_zAl_{1-z}N$-based diodes. Since impact ionization in the operation mode is at the initial stage, the valence band was represented only by the band of heavy holes. For the same reason, energy and momentum conservation laws were applied to determine the final state of charge carriers after impact ionization and to get a detailed dispersion pattern of energy and velocity. Nonparabolicity of the dispersion law was taken into account.

We considered the following scattering mechanisms: optical deformation potential (DO$^\pm$), acoustic deformation potential (DA$^\pm$), intervalley scattering between equivalent and nonequivalent valleys (Γ$^\pm$, $\Gamma_1^\pm$, M-L$^\pm$), polar optical phonon scattering (PO$^\pm$), piezoelectric scattering (PZ), alloy disorder scattering (AD), ionized-impurity scattering (I). Here, the upper (lower) sign in the superscript denotes phonon absorption (emission). The calculation details correspond to [15-18]. Material parameters were chosen according to [19, 20]. The scattering time was determined by the numerical solution of the integral equation for each particle at time t.

A 2D-model of the diode was considered, in which the diode area was represented by a rectangle. To take into account the anisotropy of material properties and the dependence of permittivity on coordinate, we solved the Poisson equation by means of full multigrid (FMG) method [16] and improved cloud-in-cell (CIC) scheme [21]. The obtained (temporary) time sample was used to estimate the noise characteristics of diodes with CSD. The numerical algorithm corresponded to [22]. NPSD $S(\omega)$ was evaluated by the autocorrelation function (ACF) of current sequences.

3. FEATURES OF KINETIC PROCESSES IN DIODES WITH CSD

On the contrary to long diodes with CSD, the characteristics of the considered elements of diodes with CSD are determined by a number of processes, including short length effects in the diode active region. On the one hand, a situation arises when electrons move through the diode active region, since only a few scattering events take place. On the other hand, it is important to obtain a high value of noise gain by maximizing shot current fluctuations as the charge passes through the diode active region.

Fig. 2 shows the distributions of the drift velocity and scattering intensity (in relative units) of electrons due to the action of individual scattering mechanisms in diodes based on $In_{1-z}Ga_zN$ with different δ at an applied bias voltage of 7 V corresponding to the diode active region.

The dominant scattering mechanism is the polar optical phonon scattering which occurs mainly in the diode active region and forms a wide spread of velocities at its output. The second significant mechanism that results in the velocity dispersion is alloy disorder scattering. The latter dominates in the region of the graded-gap layer at the cathode and forms the initial chaotic distribution of electrons at the beginning of the active region. This is the mechanism associated with the occurrence of "failure" in the velocity distribution along the diode.

The maximum value of the alloy disorder potential U_S was defined as the difference in the electronic affinity of two binary compounds which corresponds to the values 0 and 1 of the ternary material system. Among the considered diodes, the largest value of U_S corresponds to the $In_{1-z}Al_zN$-based structure.

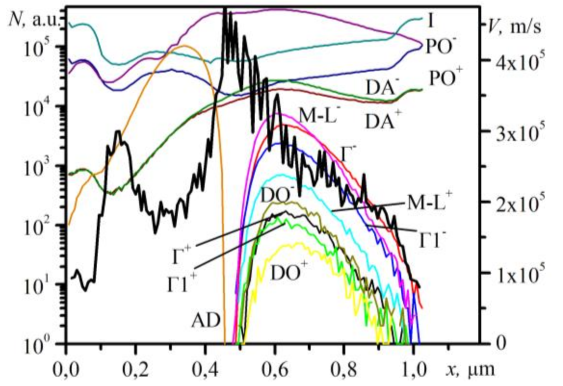

a

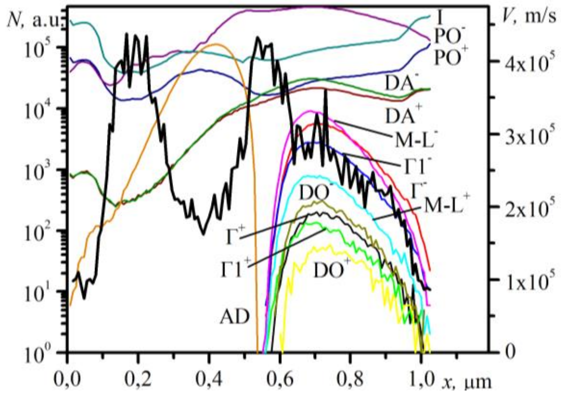

b

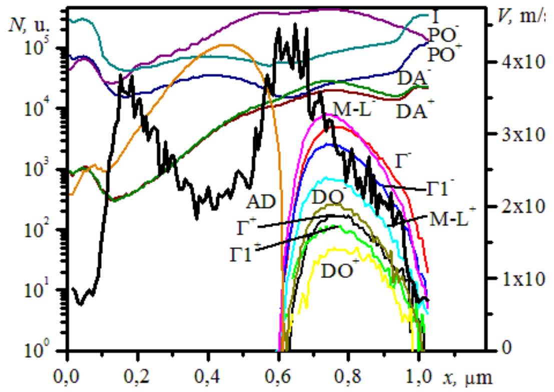

c

Fig. 2 – Dependences of the number of scattering events and mean velocity (drop line) on the coordinate for $In_zGa_{1-z}N$-based diodes at bias voltage $U = 7$ V: a) $\delta = 0.67$, b) $\delta = 1$, c) $\delta = 1.5$

The doping profile and the distribution of indium molar fraction in $In_{1-z}Al_zN$ completely correspond to diodes based on $In_zGa_{1-z}N$. For such diodes, alloy potential scattering is dominant at voltages up to 7 V. Electron energy distribution is formed under the influence of intervalley scattering and sharp intervalley electron transfer. This occurs directly in the graded-gap layer for a small In content. In general, in such diodes, the start point of intervalley transfer is shifted almost 200 nm closer to the cathode than in $In_zGa_{1-z}N$-based diodes and corresponds to the graded-gap layer end.

The coordinate dependences of the drift velocity and scattering intensity (in relative units) of the electron due to the action of individual scattering mechanisms in $In_zAl_{1-z}N$-based diodes are shown in Fig. 3. All features of the processes that are inherent in diodes based on $In_zGa_{1-z}N$ will determine the characteristics of $In_zAl_{1-z}N$ diodes. One of the features is intervalley electron transfer, which limits the velocity by the value of $v_{max} < 2.5\cdot10^5$ m/s. For this reason, the deviation from the mean velocity is less than in $In_zGa_{1-z}N$-based diodes.

Having found out that the localization of the graded-gap layer for the formation of the noise characteristics of the diode becomes essential, we studied the influence of this factor in structures where the size of the graded-gap layer was equal to the size of the reduced concentration region. We changed the position of the beginning of the graded-gap layer with respect to the end of the reduced concentration region. In particular, we considered cases when the graded-gap layer started at the beginning (type 1), at the middle (type 2) and at the end (type 3) of the reduced concentration region. The corresponding distributions of the drift velocity and intensity of electron scattering due to the action of individual scattering mechanisms for a diode of type 3 are shown in Fig. 3.

The active mode of diode operation corresponds to the initial stage of impact ionization (before breakdown). This is the main reason to form the graded band gap layer and localize impact ionization in the cathode region. As can be seen from Fig. 4, the shift of position of the graded-band gap layer leads to an increase in the velocity and its dispersion. It is also important that impact ionization becomes less sensitive.

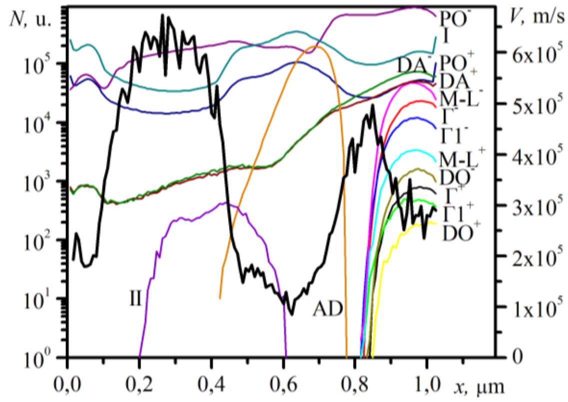

Fig. 3 – Dependences of the number of scattering events and mean velocity (drop line) on the coordinate for $In_zGa_{1-z}N$-based diodes at bias voltage $U = 7$ V, $\delta = 0.67$, the graded-gap layer begins at the end of the reduced concentration region

4. NOISE CHARACTERISTICS OF DIODES WITH CSD

Some frequency dependences of NPSD for considered diodes are shown in Fig. 5. It is seen that the dependence $S(f)$ decreases as frequency $f^{-\alpha}$ grows, where $\alpha = 1$ in the considered frequency range. All our findings support the fact that shot current fluctuations are the main source of noise generation in the diode.

At moderate bias voltages (Fig. 4) and high frequencies (above 150-200 GHz), the dependence $S(f)$ is formed under the influence of carrier scattering mechanisms in the diode, in particular, impurity scattering

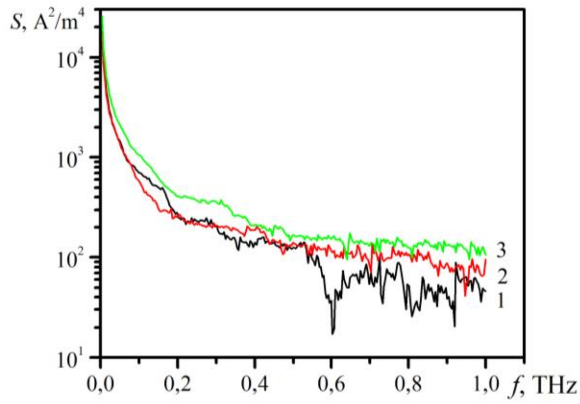

Fig. 4 – Dependences of NPSD on frequency for $In_{1-z}Ga_zN$-based diodes at bias voltage of $U = 7$ V: 1 – $\delta = 0.67$; 2 – $\delta = 1$; 3 – $\delta = 1.5$

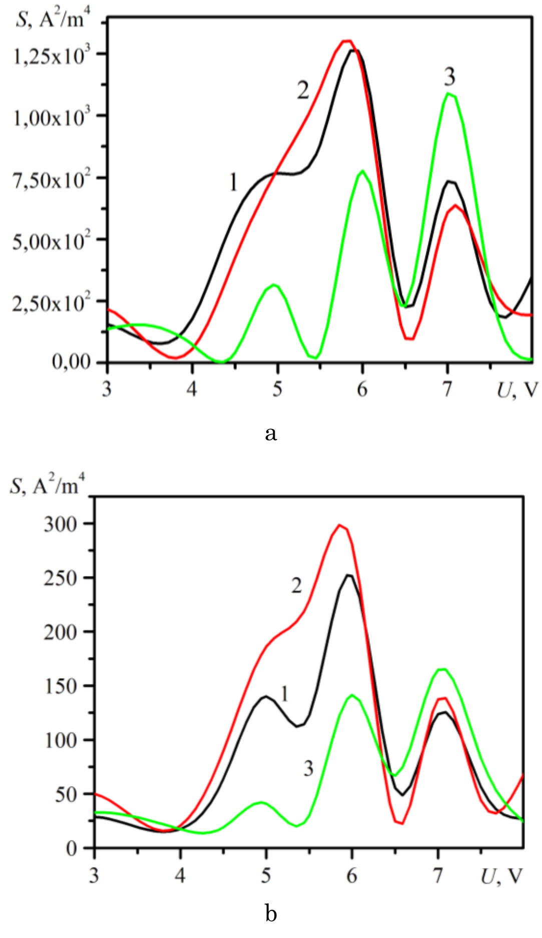

Fig. 5 – Dependences of NPSD on bias voltage for $In_{1-z}Ga_zN$-based diodes: 1 – $\delta = 0.67$, 2 – $\delta = 1$, 3 – $\delta = 1.5$; a) $f = 95$ GHz, b) $f = 0.5$ THz

and alloy potential scattering. This dependence is inherent in almost the entire frequency range. Nevertheless, we obtained somewhat different results for InAlN-based diodes, for which $a >> 0.86 \div 0.89$. This can explain the large fraction of ballistic electrons for the considered diode lengths. It should be noted that the value of NPSD increases with increasing the average current in the diode. The influence of bias voltage on noise generation is shown in Fig. 5.

The shapes of the dependences of NPSD on voltage for a certain diode are similar in a wide frequency range. There is a region with the highest NPSD value for all the diodes. The region size decreases if the maximum quasi-electric field shifts towards the anode contact. This corresponds to an increase in δ. For all InGaN-based diodes, there is a maximum of NPSD corresponding to a voltage of $U \sim 6$ V. Note that an increase in δ leads to the shape change of NPSD-voltage dependences. Thus, a sharp contrast between separate zones of noise generation is observed and takes place in InAlN-based diodes, where a number of noise generation regions are also observed.

The existence of wide bias voltage ranges where NPSD-voltage dependences are almost linear is an important property which manifests itself at rather low frequencies. In particular, for InGaN diodes with $\delta = 1$, there is a suitable voltage range from 4 to 6 V at a frequency of 95 GHz. Moreover, in this range, the change in the NPSD value is more than an order of magnitude. Thus, considered InGaN-based diodes can be used as an active voltage-controlled noise load in radiometric systems for both millimeter and THz range.

5. CONCLUSIONS

We have explored the processes associated with the electron transport effect in graded-gap III nitride-based diodes with CSD by means of Monte Carlo simulation. We have found out that the noise characteristics of the diodes are determined by the velocity distribution and the possibility of impact ionization in the region near the cathode. Moreover, we have established that alloy disorder scattering, polar optical phonon and acoustic phonon scattering are the main mechanisms to form velocity distribution. It should be noted that alloy disorder scattering dominates in InGaN-based layers.

We have shown that the best conditions for noise generation are realized when the beginning of the graded-gap layer is shifted towards the anode. In this case, the effect of speeding is more pronounced. Moreover, electrons moving in the n^--region are able to increase their energy, which is sufficient for impact ionization. Thus, optimal conditions for maximum velocity dispersion are achieved. We have established that better results can be achieved by applying the graded-gap $In_zGa_{1-z}N$ layer to the cathode contact.

The use of a nitride-based graded-gap material allows to influence the noise characteristics of the diode. We have identified wide bias voltage ranges, where NPSD-voltage dependences are almost linear, which makes it possible to develop voltage-controlled noise loads for radiometric systems in a wide frequency range.

REFERENCES

1. J.P. Crandall, J.H. O, P. Gajwani, J.P. Leal, D.D. Mawhinney, F. Sterzer, R.L. Wahl, *J. Nucl. Med.* **59** No 8, 1243 (2018).
2. D.C. Price, L.J. Greenhill, A. Fialkov, G. Bernardi, H. Garsden, B.R. Barsdell, J. Kocz, M.M. Anderson, S.A. Bourke, J. Craig, M.R. Dexter, J. Dowell, M.W. Eastwood, T. Eftekhari, S.W. Ellingson, G. Hallinan, J.M. Hartman, R. Kimberk, T.J.W. Lazio, S. Leiker, D. MacMahon, R. Monroe, F. Schinzel, G.B. Taylor, E. Tong, D. Werthimer, D.P. Woody, *Mon. Not. R. Astron. Soc.* **478** No 3, 4193 (2018).
3. H.J. Kramer, *Observation of the Earth and Its Environment: Survey of Missions and Sensors* (Berlin: Springer-Verlag: 2002).
4. C. Parashare, P. Kangaslahti, S. Brown, D. Dawson, T. Gaier, S. Padmanabhan, A. Tanner, O. Montes, V. Hadel, T. Johnson, X. Bosch-Lluis, S.C. Reising, *13th Specialist Meeting On Microwave Radiometry and Remote Sensing of the Environment (Microrad 2014)*, art. no. 14528309, 157 (Pasadena: IEEE: 2014).
5. H. Song, T. Nagatsuma, *Handbook of terahertz technologies: devices and applications* (Singapore: Pan Stanford Publishing: 2015).
6. T. Isogawa, T. Kumashiro, H. Song, K. Ajito, N. Kukutsu, K. Iwatsuki, T. Nagatsuma, *IEEE T. Te. Sci. Techn.* **2** No 5, 485 (2012).
7. W.L. Chan, J. Deibel, D.M. Mittleman, *Rep. Prog. Phys.* **70** No 8, 1325 (2007).
8. N. Ehsan, J. Piepmeier, M. Solly, S. Macmurphy, J. Lucey, E. Wollack, *2015 European Microwave Conference (EuMC)*, art. no. 15649195, 853 (Paris: IEEE: 2015).
9. I.M. Abolduev, V.V. Veytz, G.Z. Garber, A.Y. Evgrafov, A.M. Zubkov, V.M. Minnebaev, A.V. Chernykh, *Elektronnaya tekhnika. Series 2. Poluprovodnikovye pribory* **230** No 1, 22 (2013) [In Russian].
10. D.E. Radchenko, V.I. Kalinin, V.D. Kotov, V.E. Lyubchenko, S.V. Marechek, S.A. Telegin, E.O. Yunevich, *Zhurnal Radioelektroniki* No 12, 5 (2019) [In Russian].
11. E.D. Prohorov, S.N. Skorobogatova, *Sov. J. Com. Tech. Electron.* **30** No 7, 14447 (1985).
12. I.P. Storozhenko, M.V. Kaydash, *J. Nano- Electron. Phys.* **10** No 4, 04014 (2018).
13. I.P. Storozhenko, *Telecomm. Radio Eng+* **75** No 12, 1101 (2016).
14. O.V. Botsula, K.H. Pryhodko, V.A. Zozulia, *J. Nano- Electron. Phys.* **11** No 1, 01006 (2019).
15. E.D. Prokhorov, O.V. Botsula, A.V. Dyadchenko, I.A. Gorbunov, *23rd Int. Crimean Conference "Microwave & Telecommunication Technology" (CriMiCo'2013)*, art. no. 13882550, 139 (Sevastopol: IEEE: 2013).
16. W. Joppich, S. Mijalkovic, *Multigrid Methods for Process simulation* (Wien, New York: Springer-Verlag: 1993).
17. K. Brennan, N. Mansour, *J. Appl. Phys.* **69** No 11, 7844 (1991).
18. K.H. Prykhodko, V.O. Zozulia, O.V. Botsula, *2017 IEEE International Young Scientists Forum on Applied Physics and Engineering (YSF–2017)*, art. no. 17413958, 291, (Lviv: IEEE:2017).
19. H. Morkoc, *Handbook of Nitride Semiconductors and Devices*, (Weinheim: Wiley-VCH: 2009).
20. P. Siddiqua, W.A. Hadi, M.S. Shur, S.K. O'Leary, *J. Mater. Sci.-Mater. El.* **26**, 4475 (2015).
21. S.E. Laux "On particle-mesh coupling on Monte Carlo device simulation, *IEEE T. Comput. Aid. D.* **15** No 10, 1266 (1996).
22. O.V. Botsula, K.H. Pryhodko, *Telecomm. Radio Eng+* **76** No 10, 891 (2017).

Особливості генерації шуму в діодах на основі нітридних сполук з варізонним шаром

К.Г. Приходько[1], С.В. Плаксін[2]

[1] *Харківський національний університет імені В.Н. Каразіна, площа Свободи, 4, 61077 Харків, Україна*

[2] *Інститут транспортних систем і технологій «Трансмаг» НАН України, вул. Писаржевського, 5, 49005 Дніпро, Україна*

Діоди з варізонним шаром із статичним доменом сильного поля розглядаються як можливе джерело шуму для сучасних застосувань, які використовують частоти терагерцового діапазону. Діоди являють собою двоконтактну $n^+–n^-–n–n^+$ структуру, яка містить катодний варізонний шар із енергетичним зазором, що зростає від катодного контакту до початку n-області. Розглянуто діоди на основі GaN та AlN відповідно із зазорами на основі $In_zGa_{1-z}N$ та $In_zAl_{1-z}N$. Завдяки використанню варізонного шару з вузькозонним матеріалом на катоді досягається локалізація сильного електричного поля та низьке значення порогу ударної іонізації. Моделювання діодів було виконано багаточастинковим методом Монте-Карло. Генерація шуму досліджується шляхом числового аналізу часових вибірок електричного струму в часовій області. Досліджено вплив механізмів розсіювання, що діють на носії заряду, на шумові властивості діода. Аналізується щільність потужності спектрального шуму (NPSD). Виявлено, що максимальна NPSD спостерігається в діодах GaN з шаром $In_zGa_{1-z}N$. Величина NPSD залежить від розмірів як n^- області (на фіксованій довжині діода), так і положення варізонного шару відносно кінця області з високим опором (n^-). Встановлено, що розсіювання на полярних фононах та розсіювання на сплаві є основними механізмами, які впливають на шумові властивості діодів. Показано, що діоди демонструють області у напрузі зміщення, в яких залежність NPSD від напруги є лінійною, а величина NPSD змінюється більше ніж на порядок.

Ключові слова: Катодний статичний домен, Варізонний шар, Ударна іонізація, Генерація шуму, Розсіяння, Спектральна щільність потужності шуму.